Magnetic anisotropy of ferromagnetic $Ga_{1-x}Mn_xAs$ formed by Mn ion implantation and pulsed-laser melting

Y. J. Cho,[1,a)] M. A. Scarpulla,[2,3,b)] Y. Y. Zhou,[1] Z. Ge,[1] X. Liu,[1] M. Dobrowolska,[1] K. M. Yu,[3] O. D. Dubon,[2,3] and J. K. Furdyna[1]
[1]*Department of Physics, University of Notre Dame, Notre Dame, Indiana 46556, USA*
[2]*Department of Materials Science and Engineering, University of California, Berkeley, California 94720, USA*
[3]*Lawrence Berkeley National Laboratory, Berkeley, California 94720, USA*

(Received 3 May 2008; accepted 10 June 2008; published online 18 August 2008)

We measured the magnetic anisotropy of nearly fully relaxed ferromagnetic $Ga_{1-x}Mn_xAs$ formed by Mn ion implantation followed by pulsed-laser melting (II-PLM) using magnetometry and ferromagnetic resonance. In qualitative terms the material formed by II-PLM exhibits all magnetic anisotropy features commonly found in $Ga_{1-x}Mn_xAs$ films fabricated by low-temperature molecular beam epitaxy (LT-MBE). Quantitatively, however, the magnetic anisotropy of II-PLM $Ga_{1-x}Mn_xAs$ is dominated by cubic anisotropy terms, which we attribute to the smaller strain in the II-PLM material due to the absence of Mn interstitials. One should note, however, that II-PLM $Ga_{1-x}Mn_xAs$ also exhibits a weak but finite uniaxial in-plane magnetic anisotropy similar to that observed in LT-MBE $Ga_{1-x}Mn_xAs$, which can be ascribed to the small built-in compressive strain. The similarity between II-PLM and LT-MBE $Ga_{1-x}Mn_xAs$ clearly points to an intrinsic origin of this property, independent of the method of fabrication. At low temperatures the remnant in-plane magnetization of the II-PLM film exhibits single-domain characteristics, while perpendicular magnetization shows a multiple-domain behavior. © *2008 American Institute of Physics*. [DOI: 10.1063/1.2966598]

I. INTRODUCTION

As a strong candidate of spintronic devices, ferromagnetic $Ga_{1-x}Mn_xAs$ continues to be intensely investigated.[1,2] It has been known since early works that $Ga_{1-x}Mn_xAs$ films show a rather strong strain induced magnetic anisotropy.[3] However, the understanding of the magnetic anisotropy of $Ga_{1-x}Mn_xAs$ is far from complete. Although many magnetic anisotropy studies of $Ga_{1-x}Mn_xAs$ have been performed with films exclusively grown by low-temperature molecular beam epitaxy (LT-MBE),[4–7] its inherent defects [e.g., Mn interstitials (Mn_I) and As antisites (As_{Ga})] might unintentionally result to extrinsic magnetic anisotropy. In this work, we report on the magnetic anisotropy of a ferromagnetic $Ga_{1-x}Mn_xAs$ film synthesized by Mn ion implantation into GaAs followed by pulsed-laser melting (II-PLM) and compare its properties to the results obtained in an as-grown LT-MBE $Ga_{1-x}Mn_xAs$ ($x=0.05$) epilayer. This sample was chosen for the purpose of comparison because its Curie temperature ($T_C \sim 60$ K) is close to that of II-PLM film.

II. SAMPLE PREPARATION

A semi-insulating GaAs (001) wafer was implanted with 80 keV Mn ions to a dose of $1\times10^{16}/cm^2$. The implanted sample was irradiated in air with a single 0.45 J/cm^2 pulse from a KrF excimer laser (248 nm, ~30 ns), causing the implanted layer to first melt and then crystallize upon solidification. The rapid submicrosecond melting and solidification associated with laser processing lead to a high level of Mn incorporation in the regrown single crystalline layer while suppressing the formation of second phases. The detailed procedure of this method of synthesis is described elsewhere.[8,9] Secondary ion mass spectrometry shows that although the Mn concentration varies in depth, the significant Mn concentrations are confined to a thickness of approximately 100 nm from the surface in the film discussed in this work.[8] Films synthesized by II-PLM under these conditions are characterized by a peak in the concentration of the substitutional Mn (Mn_{Ga}) of ~2.4 %, i.e., $Ga_{0.976}Mn_{0.024}As$.

III. RESULTS AND DISCUSSION

The structure of the film and the position of Mn in the lattice were evaluated using channeling Rutherford backscattering spectrometry and particle-induced x-ray emission (PIXE) with 1.95 MeV $^4He^+$. There is no difference in PIXE yields within experimental error along the [110] and [111] directions (not shown), reflecting the fact that Mn_I defects are absent in films formed by II-PLM.[8,10] Figure 1 shows the x-ray diffraction (XRD) rocking curves for the (004) reflection of the $Ga_{0.976}Mn_{0.024}As$ formed by II-PLM. For comparison the XRD of a $Ga_{0.95}Mn_{0.05}As$ epilayer grown by LT-MBE is shown in the inset of Fig. 1. Unlike the LT-MBE epilayer, the II-PLM $Ga_{1-x}Mn_xAs$ film does not show a clear peak but only a small shoulder on the left side of the GaAs(001) substrate peak (see Fig. 1), indicating that the film contains only a small compressive strain.

Field dependent magnetization $M(H)$ at $T=5$ K and temperature dependent remnant magnetization $M_R(T)$ measured on the II-PLM sample using a superconducting quan-

[a)]Electronic mail: ycho1@nd.edu.
[b)]Present address: Materials Department, University of California, Santa Barbara, California 93106, USA.

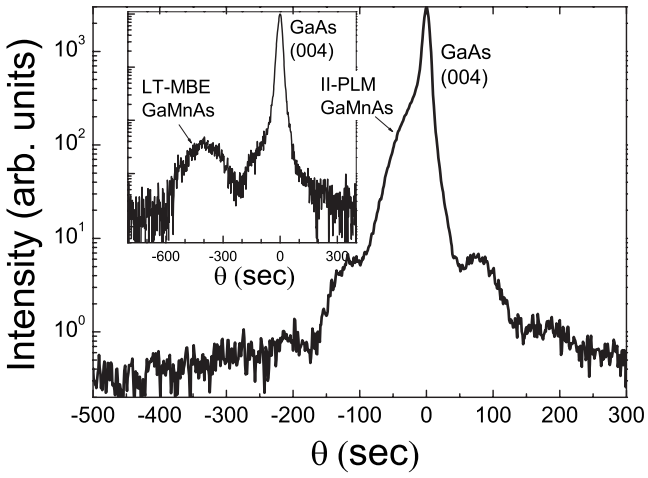

FIG. 1. XRD rocking curve of the (004) reflection for the II-PLM formed $Ga_{0.976}Mn_{0.024}As$ film. The strongest peak corresponds to the GaAs substrate. Inset: XRD rocking curve for the (004) reflection of a 100 nm LT-MBE grown $Ga_{0.95}Mn_{0.05}As$ with $T_C \sim 60$ K, shown for comparison.

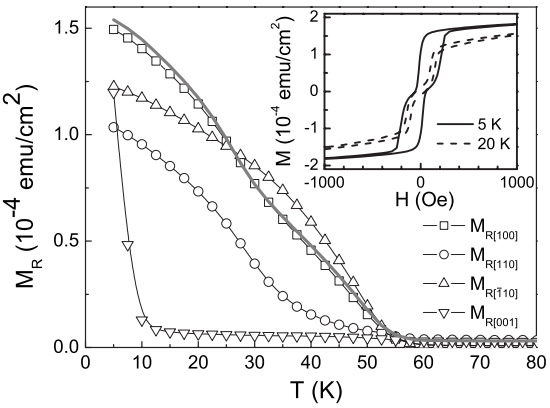

FIG. 3. Temperature dependence of remnant magnetization (M_R) of the II-PLM $Ga_{1-x}Mn_xAs$ sample along the [110], [$\bar{1}$10], [001], and [100] directions. The thick gray line shows $M_{R[100]}$ extracted from the measured $M_{R[110]}$ and $M_{R[\bar{1}10]}$ by assuming single-domain behavior for in-plane magnetization. Inset: Magnetization vs field along [001] at $T=5$ and 20 K for the II-PLM $Ga_{1-x}Mn_xAs$ sample.

tum interference device (SQUID) magnetometer are shown in Figs. 2 and 3, respectively. The T_C of this specimen is ~60 K. As was already mentioned, the II-PLM sample has a negligible concentration of Mn_I. If we assume that there are no compensating defects, the hole concentration p can then be assumed to be close to the Mn concentration. Using $x=0.024$, this yields $p \sim 5 \times 10^{20}/cm^3$. It is interesting that if one applies the *p-d* Zener model to this sample, one obtains T_C to be ~65 K, a value that is rather close to the measured value of T_C, ~60 K. Within experimental error it was found that there is no difference in magnetization along the the [100] and [010] directions. However, it is clearly seen that magnetization along the [110] direction is different from that along [$\bar{1}$10], similar to the results observed in $Ga_{1-x}Mn_xAs$ grown by LT-MBE. This indicates an *intrinsic* in-plane uniaxial magnetic anisotropy component that is unrelated to the biaxial compressive strain. Moreover, as seen in Fig. 3, the temperature dependence of the in-plane magnetization is also very similar to that found in LT-MBE grown $Ga_{1-x}Mn_xAs$ film, where the magnetic easy axis was observed to switch from the in-plane [100] to the in-plane [$\bar{1}$10] with increasing temperature.[4–7] Assuming the single-domain behavior in the (001) plane, we have extracted the magnetization along the in-plane [100] direction from the [110] and [$\bar{1}$10] components of the remnant magnetizations $M_{R[110]}$ and $M_{R[\bar{1}10]}$. The result is shown as a thick gray line in Fig. 3 and is in very good agreement with the value of $M_{R[100]}$ obtained by direct measurement. One should also note (see Fig. 3) that the out-of-plane remnant magnetization $M_{R[001]}$ goes to a near-zero value for $T \geq 10$ K. These magnetization measurements indicate the existence of an in-plane cubic and uniaxial anisotropy terms in the II-PLM formed $Ga_{0.976}Mn_{0.024}As$ film. These two anisotropy terms exhibit the same features as those observed in LT-MBE $Ga_{1-x}Mn_xAs$ films, which suggests that the origin of the in-plane cubic and the uniaxial anisotropies is closely related to the undistorted GaAs crystal structure.

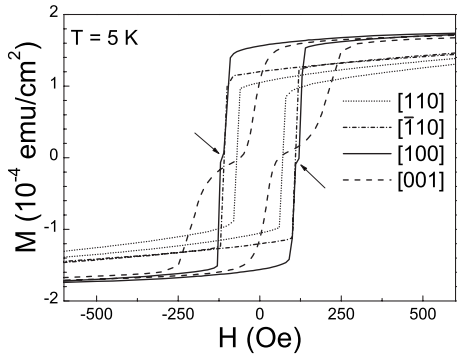

FIG. 2. Magnetization as a function of applied magnetic field observed on the II-PLM $Ga_{1-x}Mn_xAs$ film measured at $T=5$ K for magnetic field applied parallel to [110], [$\bar{1}$10], [001], and [100]. The arrows point to the small kinks due to double jumps observed in the case of $M_{[100]}$.

Figure 2 demonstrates that—unlike the case of LT-MBE $Ga_{1-x}Mn_xAs$—in II-PLM $Ga_{1-x}Mn_xAs$, the [001] direction is also one of the easy axes. This can be seen from the hysteresis loop for $M(H)$ along [001], which reaches full saturation at ~500 Oe, only slightly more than the saturation field for $M_{[100]}$ and far less than that for the in-plane [$\bar{1}$10] and [110] directions. (The similarity of the three ⟨100⟩ axes is further brought out by the fact that saturation in all three cases is reached by a two 90° rotation process evidenced by the two kinks in the hysteresis, even though this is quantitatively somewhat different for the [001] and the in-plane ⟨100⟩ orientations. This point will be discussed later.)

To gain a better understanding of the magnetic anisotropy in the II-PLM material, we performed ferromagnetic resonance (FMR) on this specimen. The FMR measurements were carried out at 9.46 GHz using a Bruker electron paramagnetic resonance spectrometer. The sample was placed in a Suprasil tube inserted in a liquid helium continuous flow cryostat, which could achieve temperatures down to 4.0 K. The detailed procedure used in FMR measurements on $Ga_{1-x}Mn_xAs$ films is described in Ref. 5. In the present work we will focus on the dependence of the FMR position on the orientation of the applied field H in four planes: (1$\bar{1}$0), (110),

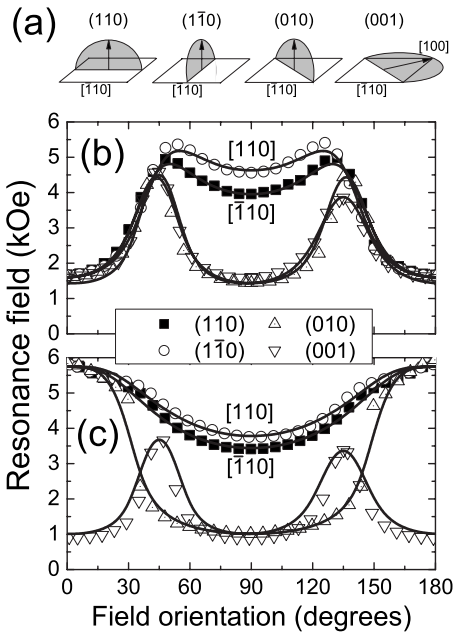

FIG. 4. Angular dependence of FMR fields for $\boldsymbol{H}$ and $\boldsymbol{M}$ in the (110), ($\bar{1}$10), (010), and (001) planes, respectively. (a) Schematic diagrams showing the four geometries in which the field orientation is varied. (b) Angular dependence of FMR fields for II-PLM $Ga_{0.976}Mn_{0.024}As$. (c) Angular dependence of FMR for LT-MBE $Ga_{0.95}Mn_{0.05}As$ film. The solid curves in the figure are theoretical fits to the observed FMR fields. Note the inequivalence of the [110] and [$\bar{1}$10] data, clearly seen in the FMR data for both II-PLM and LT-MBE specimens.

(010), and (001), as shown schematically in Fig. 4(a). In Figs. 4(b) and 4(c) we plot the angular dependence of FMR at 4 K observed on II-PLM $Ga_{0.976}Mn_{0.024}As$ and LT-MBE $Ga_{0.95}Mn_{0.05}As$ films, respectively. As can be seen in Fig. 4, both specimens show a clear in-plane uniaxial anisotropy, which reflects the fact that [110] and [$\bar{1}$10] are not magnetically equivalent. This result again suggests that the in-plane uniaxial anisotropy of the $Ga_{1-x}Mn_xAs$ system is not simply a by-product of LT-MBE growth.

To obtain the magnetic anisotropy fields from FMR data, we write the free energy density F for a thin film with zinc-blende structure under a slight tetragonal distortion in the presence of an applied magnetic field H,[5]

$$F = -MH[\cos\theta\cos\theta_H + \sin\theta\sin\theta_H\cos(\varphi-\varphi_H)] + \frac{1}{2}MH_{\text{eff}}\cos^2\theta - \frac{1}{4}MH_{4\perp}\cos^4\theta - \frac{1}{4}MH_{4\parallel}\frac{1}{4}(3+\cos 4\varphi)\sin^4\theta - \frac{1}{2}MH_{2\parallel}\sin^2\theta\sin^2\left(\varphi-\frac{\pi}{4}\right). \quad (1)$$

Here the first term describes the Zeeman energy; H_{eff} corresponds to the effective field normal to the layer that includes both demagnetization and perpendicular uniaxial anisotropy fields; $H_{2\perp}$ ($H_{2\parallel}$) and $H_{4\perp}$ ($H_{4\parallel}$) represent the perpendicular (in-plane) uniaxial and perpendicular cubic anisotropy fields, respectively; θ and θ_H are the angles measured from [001] to $\boldsymbol{M}$ and $\boldsymbol{H}$, respectively; and φ and φ_H are the angles from

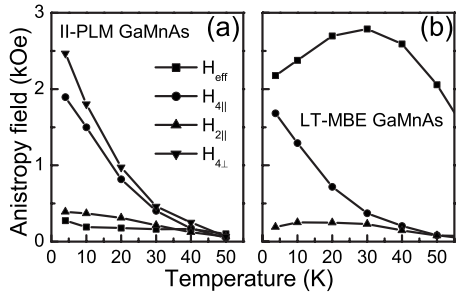

FIG. 5. Magnetic anisotropy fields plotted as a function of temperature for II-PLM and LT-MBE samples. (a) Data for II-PLM $Ga_{0.976}Mn_{0.024}As$ sample. (b) Data for $Ga_{0.95}Mn_{0.05}As$ grown by LT-MBE. Note that $H_{4\perp}$ is nearly zero for LT-MBE $Ga_{1-x}Mn_xAs$ (too small to be seen on the scale of the figure).

[100] to the projection of $\boldsymbol{M}$ and $\boldsymbol{H}$ on the (001) plane, respectively.

Using the fitting procedure described in Ref. 5, the five parameters obtained for the II-PLM $Ga_{1-x}Mn_xAs$ sample are $H_{\text{eff}}=308$ Oe, $H_{4\perp}=2535$ Oe, $H_{4\parallel}=1974$ Oe, $H_{2\parallel}=394$ Oe, and $g=1.86$. The resulting fits to the FMR data for the II-PLM sample are shown as solid curves in Fig. 4(b). For comparison, we also show the FMR data for the LT-MBE $Ga_{0.95}Mn_{0.05}As$ specimen along with their theoretical fits in Fig. 4(c), and we list the resulting anisotropy parameters for LT-MBE $Ga_{1-x}Mn_xAs$: $H_{\text{eff}}=2145$ Oe, $H_{4\perp}=105$ Oe, $H_{4\parallel}=1653$ Oe, $H_{2\parallel}=192$ Oe, and $g=1.87$.

These results reveal two obvious differences between the II-PLM and LT-MBE materials. First, the value of the perpendicular uniaxial anisotropy in the II-PLM $Ga_{1-x}Mn_xAs$ specimen is far smaller than the value of the cubic term in this specimen and is also much smaller than the corresponding term in the LT-MBE $Ga_{1-x}Mn_xAs$ specimen. Second, the two cubic terms in II-PLM $Ga_{1-x}Mn_xAs$ are of comparable magnitude. This second observation is very different from the behavior seen in the case of the LT-MBE grown material, where $H_{4\parallel} \gg H_{4\perp}$ and $H_{4\perp} \sim 0$. These two differences are consistent with the fact that the effects of compressive strain in II-PLM $Ga_{1-x}Mn_xAs$ are far weaker than those in the LT-MBE grown samples. Additionally, the low built-in strain in the II-PLM specimen leads to clear differences in the angular dependences of the FMR field observed on II-PLM and LT-MBE specimens in the three planes [i.e., (1$\bar{1}$0), (110), and (010)], as seen in the plots in Fig. 4. For completeness, in Figs. 5(a) and 5(b) we also show the temperature dependence of the anisotropy fields for the II-PLM and LT-MBE specimens, respectively. Clearly, in contrast to the two perpendicular anisotropy terms, the two in-plane anisotropy fields $H_{2\parallel}$ and $H_{4\parallel}$ show similar temperature dependences in the two specimens.

Finally, a clear *two-jump* magnetization reversal process is evident for the [001] direction (see inset in Fig. 3), which is commonly observed when cubic anisotropy competes with uniaxial anisotropy.[11–13] As for the [100] direction, only two very small kinks are seen around $M_{[100]} \sim 0$ (marked by arrows in Fig. 2), indicating that the two 90° jumps occur within very narrow field windows (about 25 Oe) for that orientation of $\boldsymbol{M}$. The fact that the field change required to

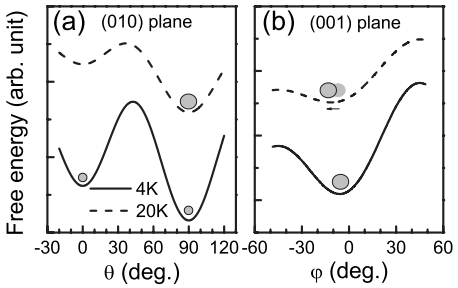

FIG. 6. [(a) and (b)] Plots of angular dependence of free energy for the II-PLM $Ga_{1-x}Mn_xAs$ for $\boldsymbol{M}$ in the (010) and (001) planes at $T=4$ and 20 K obtained via Eq. (1). The angles θ and φ are measured from the [001] and [100] directions, respectively. Note that the [100] and [010] directions are equivalent.

achieve the two 90° jumps in the $M_{[001]}$ reversal is about an order of magnitude greater than that for $M_{[100]}$ suggests that the evolution of domains during the process of perpendicular magnetization reversal is different from that happening during in-plane magnetization reversal. If the magnetization $\boldsymbol{M}$ in the sample is assumed to be in a single-domain state, then it follows from the 5 K data in Fig. 3 that the angle between $\boldsymbol{M}$ and the [001] direction [i.e., the angle θ in Eq. (1)] must be ~42°.

To obtain a better picture of whether $\boldsymbol{M}$ in the sample exists in a single or multiple form, we plot in Fig. 6 the angular dependence of the free energy at $\boldsymbol{H}=0$ Oe obtained via Eq. (1) using magnetic anisotropy fields from the FMR fits, which shows the free energy minima as a function of the orientation of $\boldsymbol{M}$. The angles θ and φ are defined below Eq. (1). We see from Fig. 6(a) that the free energy at $\theta \sim 42°$ (i.e., close to the out-of-plane [011] orientation) is much higher than those for any of the ⟨100⟩ directions (i.e., for either $\theta = 0$ or 90° in the figure). From this we infer that the measured $M_{R[001]}$ at 5 K is a resultant magnetization of a multidomain state. This suggests that although there is a significant energy barrier between $M_{[001]}$ and $M_{[100]}$, a considerable number of domains with $\boldsymbol{M}$ close to the in-plane ⟨100⟩ directions are nucleated by thermal activation energy as $\boldsymbol{H}$ goes to zero after the $\boldsymbol{H}\|[001]$ sweep. However, since some $M_{[001]}$ domains still remain (i.e., they do not follow the nucleated domains with in-plane $\boldsymbol{M}$ via domain expansion process), this leads us to believe that the domain wall pinning energy opposing 90° changes in $\boldsymbol{M}$ is very large in II-PLM $Ga_{1-x}Mn_xAs$. However, the vanishing of $M_{R[001]}$ above 10 K, as seen in Fig. 3, indicates that above that temperature practically all domains with perpendicular $\boldsymbol{M}$ are removed, thus suggesting that above ~10 K the domain wall pinning energy is overcome by anisotropy and thermal energies.

Figure 6(b) sheds valuable light on the behavior of in-plane magnetization during the reversal process. Since there are no energy barriers between $M_{[100]}$ and either $M_{[110]}$ or $M_{[\bar{1}10]}$, a single-domain state will be formed as $\boldsymbol{H}$ goes to zero after the $\boldsymbol{H}\|[100]$, $\boldsymbol{H}\|[110]$, or $\boldsymbol{H}\|[\bar{1}10]$ sweep. We note parenthetically that, in principle, when $\boldsymbol{H}$ is applied exactly along [110] ($[\bar{1}10]$), it would be possible for the sample to break up into $M_{[100]}$ and $M_{[010]}$ ($M_{[\bar{1}10]}$ and $M_{[010]}$) domains at remanence. It was shown in recent experiments, however, that to achieve such an in-plane multidomain situation, the applied field must be within ~0.5° from one of the in-plane ⟨110⟩ directions[14]—an extremely stringent requirement in routine magnetization measurements. Since there is always some small misalignment, the ⟨110⟩ sweeps are expected to predominantly favor one of the ⟨100⟩ orientations, thus resulting in an essentially single-domain behavior. One should note, however, that as temperature increases, the barrier height between the $\varphi=0$ and $\varphi=-90°$ gradually decreases [see dashed curve in Fig. 6(b)], and the in-plane single-domain state is gradually expected to follow these temperature-induced changes in anisotropy energy, as indicated by the small arrow in Fig. 6(b). The features discussed above are reflected by the excellent agreement between the measured $M_{R[100]}$ and the values of $M_{R[100]}$ extracted from the superposition of $M_{R[110]}$ and $M_{R[\bar{1}10]}$, as seen in Fig. 3.

IV. CONCLUSIONS

The study of magnetic anisotropy carried out by SQUID magnetometry and FMR spectroscopy on a relaxed film formed by II-PLM leads us to the following conclusions. (1) In qualitative terms the II-PLM $Ga_{1-x}Mn_xAs$ film exhibits all of the magnetic anisotropy features found in as-grown LT-MBE $Ga_{1-x}Mn_xAs$ with a similar T_C, including the presence of an in-plane uniaxial anisotropy that is responsible for a difference in magnetizations along the [110] and $[\bar{1}10]$ directions. This leads us to the important conclusion that the in-plane symmetry breaking between the [110] and $[\bar{1}10]$ directions is not a consequence of MBE growth but is an *intrinsic* property of $Ga_{1-x}Mn_xAs$ films generally. (2) Quantitatively, the magnetic anisotropy of II-PLM $Ga_{1-x}Mn_xAs$ film is dominated by cubic anisotropy terms, while the uniaxial anisotropy terms are relatively weak in this material. We attribute this to the small lattice mismatch in the II-PLM film, and thus a smaller degree of compressive strain on the (001) plane as compared to the case of LT-MBE $Ga_{1-x}Mn_xAs$ with a similar T_C. Also, (3) the domain wall pinning energy for the [001] direction in II-PLM $Ga_{1-x}Mn_xAs$ is quite significant. This property results in the formation of multiple ⟨100⟩ domains in II-PLM $Ga_{1-x}Mn_xAs$ in the magnetization reversal of $\boldsymbol{M}\|[001]$, while the process of in-plane magnetization reversal (e.g., $\boldsymbol{M}\|[100]$) can be satisfactorily understood in terms of single-domain behavior in this material.

ACKNOWLEDGMENTS

The synthesis of films by II-PLM at the Lawrence Berkeley National Laboratory was supported by the Director, Office of Science, Office of Basic Energy Sciences, Division of Materials Sciences and Engineering of the U.S. Department of Energy (Contract No. DE-AC02-05CH11231). The work at Notre Dame was supported by the National Science Foundation (Grant No. DMR06-03752).

[1] H. Ohno, Science **281**, 951 (1998).
[2] T. Jungwirth, J. Sinova, J. Masek, J. Kucera, and A. H. MacDonald, Rev. Mod. Phys. **78**, 809 (2006).
[3] H. Ohno, J. Magn. Magn. Mater. **200**, 110 (1999).
[4] U. Welp, V. K. Vlasko-Vlasov, X. Liu, J. K. Furdyna, and T. Wojtowicz,

Phys. Rev. Lett. **90**, 167206 (2003).
[5]X. Liu and J. K. Furdyna, J. Phys.: Condens. Matter **18**, R245 (2006).
[6]K. Hamaya, T. Taniyama, Y. Kitamoto, R. Moriya, and H. Munekata, J. Appl. Phys. **94**, 7657 (2003).
[7]M. Sawicki, F. Matsukura, A. Idziaszek, T. Dietl, G. M. Schott, C. Ruester, C. Gould, G. Karczewski, G. Schmidt, and L. W. Molenkamp, Phys. Rev. B **70**, 245325(R) (2004).
[8]M. A. Scarpulla, R. Farshchi, P. R. Stone, R. V. Chopdekar, K. M. Yu, Y. Suzuki, and O. D. Dubon, J. Appl. Phys. **103**, 073913 (2008).
[9]M. A. Scarpulla, O. D. Dubon, K. M. Yu, O. Monteiro, M. R. Pillai, M. J. Aziz, and M. C. Ridgway, Appl. Phys. Lett. **82**, 1251 (2003).
[10]K. M. Yu, W. Walukiewicz, T. Wojtowicz, I. Kuryliszyn, X. Liu, Y. Sasaki, and J. K. Furdyna, Phys. Rev. B **65**, 201303 (2002).
[11]X. Liu, W. L. Lim, L. V. Titova, M. Dobrowolska, J. K. Furdyna, M. Kutrowski, and T. Wojtowicz, J. Appl. Phys. **98**, 063904 (2005).
[12]L. V. Titova, M. Kutrowski, X. Liu, R. Chakarvorty, W. L. Lim, T. Wojtowicz, J. K. Furdyna, and M. Dobrowolska, Phys. Rev. B **72**, 165205 (2005).
[13]E. Ahmad, L. Lopez-Diaz, E. Gu, and J. A. C. Bland, J. Appl. Phys. **88**, 354 (2000).
[14]D. Y. Shin, S. J. Chung, S. Lee, X. Liu, and J. K. Furdyna, Phys. Rev. Lett. **98**, 047201 (2007).